materials

MDPI

Article

Efficiency Improvement of Industrial Silicon Solar Cells by the $POCl_3$ Diffusion Process

Xiaodong Xu [1], Wangping Wu [1,*] and Qinqin Wang [2,*]

[1] Electrochemistry and Corrosion Laboratory, School of Mechanical Engineering, Changzhou University, Changzhou 213164, China
[2] School of Mechanical Engineering, Yangzhou University, Yangzhou 225127, China
* Correspondence: wwp3.14@163.com or wuwping@cczu.edu.cn (W.W.); wangqinqin@yzu.edu.cn (Q.W.)

Abstract: To improve the efficiency of polycrystalline silicon solar cells, process optimization is a key technology in the photovoltaic industry. Despite the efficiency of this technique to be reproducible, economic, and simple, it presents a major inconvenience to have a heavily doped region near the surface which induces a high minority carrier recombination. To limit this effect, an optimization of diffused phosphorous profiles is required. A "low-high-low" temperature step of the $POCl_3$ diffusion process was developed to improve the efficiency of industrial-type polycrystalline silicon solar cells. The low surface concentration of phosphorus doping of 4.54×10^{20} atoms/cm^3 and junction depth of 0.31 µm at a dopant concentration of $N = 10^{17}$ atoms/cm^3 were obtained. The open-circuit voltage and fill factor of solar cells increased up to 1 mV and 0.30%, compared with the online low-temperature diffusion process, respectively. The efficiency of solar cells and the power of PV cells were increased by 0.1% and 1 W, respectively. This $POCl_3$ diffusion process effectively improved the overall efficiency of industrial-type polycrystalline silicon solar cells in this solar field.

Keywords: polycrystalline silicon; solar cells; low-high-low; phosphorus diffusion

Citation: Xu, X.; Wu, W.; Wang, Q. Efficiency Improvement of Industrial Silicon Solar Cells by the $POCl_3$ Diffusion Process. *Materials* **2023**, *16*, 1824. https://doi.org/10.3390/ma16051824

Academic Editor: Cristobal Voz

Received: 31 December 2022
Revised: 18 February 2023
Accepted: 21 February 2023
Published: 23 February 2023

1. Introduction

Carbon-neutral development strategies have a significant impact on the Earth's environment, and silicon (Si) solar cells have attracted much attention as a means to use solar energy to convert sunlight into electricity [1,2]. However, a compromise between cost reduction and efficiency improvement must be reached [3]. The PN junction is one of the key technologies in crystalline Si solar cells, which affects photoelectric conversion efficiency. Therefore, the PN junction has excellent performance and stable uniformity. To improve the photoelectric conversion efficiency, the high sheet resistance of over 90 Ω/sq, which has low surface doping concentration and a shallow junction process, was accepted [4]. High open-circuit voltage (V_{oc}) and short-circuit current (J_{sc}) values were obtained by this process. Tube furnace diffusion using phosphorus oxychloride ($POCl_3$) as a dopant precursor is the dominant emitter formation technology for p-type Si solar cells [5]. The majority of the PV industry currently uses $POCl_3$ diffusion to remove metal impurities, including iron [6,7]. The solar cell emitters are obtained by P (phosphorus) diffusion in p-type Si inside of a diffusion tube furnace under controlled conditions of temperature, pressure, and gas flow to form an emitter layer [3].

The photovoltaic (PV) industry has used a quartz diffusion tube furnace to form an emitter layer of the $POCl_3$ source. However, there are three flaws in this process [8]: (1) the high sheet resistance, (2) the difficulty in controlling the uniformity of high sheet resistance, and (3) the shallow junction. Many manufacturers tried to reduce the heavy inactive phosphorus concentration and the thickness of the dead zone through an additional step in the industrial process: i.e., chemical etching of the PSG layer after the phosphorus diffusion [9–11]. This solution increased the duration of the industrial process and it is expensive. A one-step diffusion process was a common method in which a single

temperature and continuous flow of dopant gas were used to deposit phosphor silicate glass (PSG) and to drive dopants to the desired depth [12]. This is a fast process but it tends to create an excessively doped emitter that deteriorates electrical performance [13]. $POCl_3$ diffusion could be performed in a two-step process: a PSG deposition step, followed by a drive-in step at variable temperature. During the process, $POCl_3$ gas is allowed in the PSG layer, and subsequently, dopants are moved deeply from the PSG layer to the Si substrate in the drive-in step [14]. Wolf et al. [5] presented the status and perspective of emitter formation by the $POCl_3$-diffusion process and discussed the diluted source and in-situ post-oxidation technological options for advanced tube furnace $POCl_3$-diffusion processes. Cui et al. [15] studied POCl3-based diffusion optimization for the formation of homogeneous emitters and the correlation with metal contact in p-type polycrystalline Si solar cells and found that the sheet resistance is high and that the P surface concentration and emitter saturation current density (J_{oe}) are low. Cho et al. [16] compared $POCl_3$ diffusion and P ion-implantation induced gettering in solar cells and found that the increase in P implantation dose improved the gettering efficiency by increasing bulk lifetime and decreasing iron concentration, but the process remained inferior to $POCl_3$ diffusion. $POCl_3$-diffused cast quasi-mono cells showed 0.4% higher efficiency due to their higher bulk lifetimes compared to P-implanted emitters. Ghembaza et al. [17] studied the optimization of P emitter formation from $POCl_3$ diffusion for p-type Si solar cells and showed that the emitter standard sheet resistances of ~60 Ω/sq and wafer uniformity <3% were obtained from the low-pressure tube furnace. Li et al. [18] investigated $POCl_3$ diffusion for the emitter layer formation of industrial Si solar cells and presented the impact of processing parameters on emitter layer formation and electrical performance.

According to the above review, P diffusion can be performed in a single step by controlling a parameter, such as temperature or time [4], or a two-step process, such as ion implantation. In this work, a "low-high-low" (LHL) diffusion process, low-high-low temperature, and three-step diffusion were used to diffuse P elements with different $POCl_3$ flows. The ECV profile, open-circuit voltage (V_{oc}), fill factor (FF), and overall efficiency of solar cells of this process were studied and simultaneously compared with the baseline using the online conventional process.

2. Experimental

P diffusion emitters were prepared on 156 × 156 mm 0.5–3 Ω·cm p-type mc-Si wafers with a thickness of ~180 μm in the quartz furnace tube. The distance between the wafers was about 2.35 mm. These wafers were vertically inserted into the quartz boat and then placed in the furnace. There were 1000 pieces per batch. There were two diffusion processes. One was the online process, and another was the LHL diffusion process. Figure 1 shows the schematic of the online and LHL diffusion processes.

Table 1 displays the process parameters of low-temperature online diffusion, namely the BKM (Best Known Method) diffusion process and the LHL diffusion process for solar cells. For the low-temperature online diffusion process, the temperature was kept at 810 °C, and the flow of $POCl_3$, O_2, and N_2 gas was 1600 mL/min, 800 mL/min, and 30,000 mL/min, respectively. For the LHL diffusion process, the first step is a low temperature and high $POCl_3$ flow diffusion. The low temperature was controlled at about 810 °C, and the flows of $POCl_3$, O_2, and N_2 gas were set at 1900 mL/min, 800 mL/min, and 30,000 mL/min, respectively. Next, the high temperature was controlled at 825 °C and the flows of $POCl_3$, O_2. and N_2 gas were fixed at 2100 mL/min, 800 mL/min, and 30,000 mL/min, respectively. Finally, a low temperature and low $POCl_3$ flow diffusion process was used. The diffusion temperature was the same as in the first step. The flows of $POCl_3$, O_2, and N_2 gas were 1600 mL/min, 800 mL/min, and 30,000 mL/min, respectively. The three-step variable-temperature diffusion LHL process is useful in the gettering process [19].

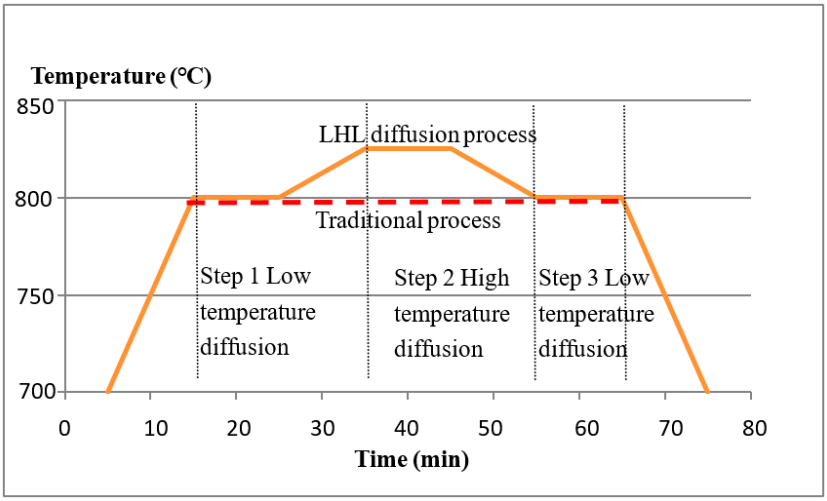

Figure 1. Schematic of BKM and LHL diffusion process.

Table 1. Process parameters of BKM and LHL diffusion processes for p-type mc-Si solar cells.

Condition		Temperature (°C)	$POCl_3$ (sccm)	O_2 (sccm)	N_2 (sccm)
BKM	1st step	810	1600	800	30,000
LHL	1st step	810	1900	800	30,000
	2nd step	825	2100	800	30,000
	Last step	:0	1600	800	30,000

Three batches of samples for each process were manufactured in order to get the average values. The sheet resistance was measured using four-point probe equipment, and the P diffusion profiles of selected samples were determined using electrochemical capacitance voltage profiling (ECV-profiling, WEP CVP21). The microstructure and morphology of the textured structure and front metalized areas were observed by scanning electronic microscopy (SEM, Quanta FEG 250, FEI). The electrical properties of solar cells were characterized by a Berger cell tester.

3. Results and Discussion

We designed the LHL diffusion process with low-high-low temperature and a three-step diffusion with different $POCl_3$ flows. The specific schematic diagrams are shown in Figure 2. Figure 2a shows the schematic diagram of the conventional primary diffusion process. Firstly, pre-oxidation is carried out with oxygen at a low temperature of 700–800 °C to generate silicon oxides on the surface of Si wafers, which is helpful to the distribution of $POCl_3$ diffusion. Then, $POCl_3$ is deposited at a low temperature of 800 °C, and finally at a high temperature of 850 °C, in order to redistribute the P element. Figure 2b presents the schematic diagram of the LHL diffusion process. LHL diffusion is characterized by three sets of P doping and three sets of redistribution. Variation in temperature is the simplest way to control the phosphorous diffusion profile. As the temperature increases, doping increases, and the formed junctions are deeper. This behavior is explained by the variation of coefficient diffusion and limited solubility with temperature. For this reason, the temperature parameter needed to achieve the necessary exact junction depth has proven to be rather delicate. With a long drive-in time, the junction is deeper. PSG deposited during the pre-deposition step acts as an infinite phosphorus source. All these results confirm that the phosphorus profile is highly affected by the tube furnace conditions. Clearly, time and temperature must be considered carefully. In this work, firstly, the pre-oxidation is carried out with oxygen at a low temperature of 800 °C. Then, the first step of low-temperature $POCl_3$ deposition is carried out, and the impurities are redistributed at variable temperatures. Subsequently, the second step of high-temperature $POCl_3$ deposition

is carried out, which is distributed with high-temperature P impurities. Finally, the third step is to deposit $POCl_3$ at a high temperature to cool down, and the impurities are redistributed. LHL diffusion process adopts low-high-low temperature and three-step diffusion with different $POCl_3$ flows. In the first step, the low temperature and high $POCl_3$ flow are the best to control the tail concentration of ECV curves. In the low-concentration tail, P diffuses into Si wafers primarily via interaction with Si self-interstitials [20,21]. In the second step, the high temperature and high $POCl_3$ flow control the kink of the slope. For high P concentration, a conversion from an interstitially to a slow vacancy-mediated process occurs, giving rise to anomalous P diffusion profiles [22]. In the third step, the low temperature and low $POCl_3$ flow can control the surface concentration of P doping. This method has the objective to decrease inactive phosphorus through an LHL step. Graphically this implies the reduction of the plateau width, which appears on the top of diffusion profiles near the high-phosphorus concentration zone. The low surface concentration of P doping could be beneficial to the V_{oc} and J_{sc} values of solar cells. However, it influences series resistance and FF values. Therefore, it is important to weigh the benefits against the risks.

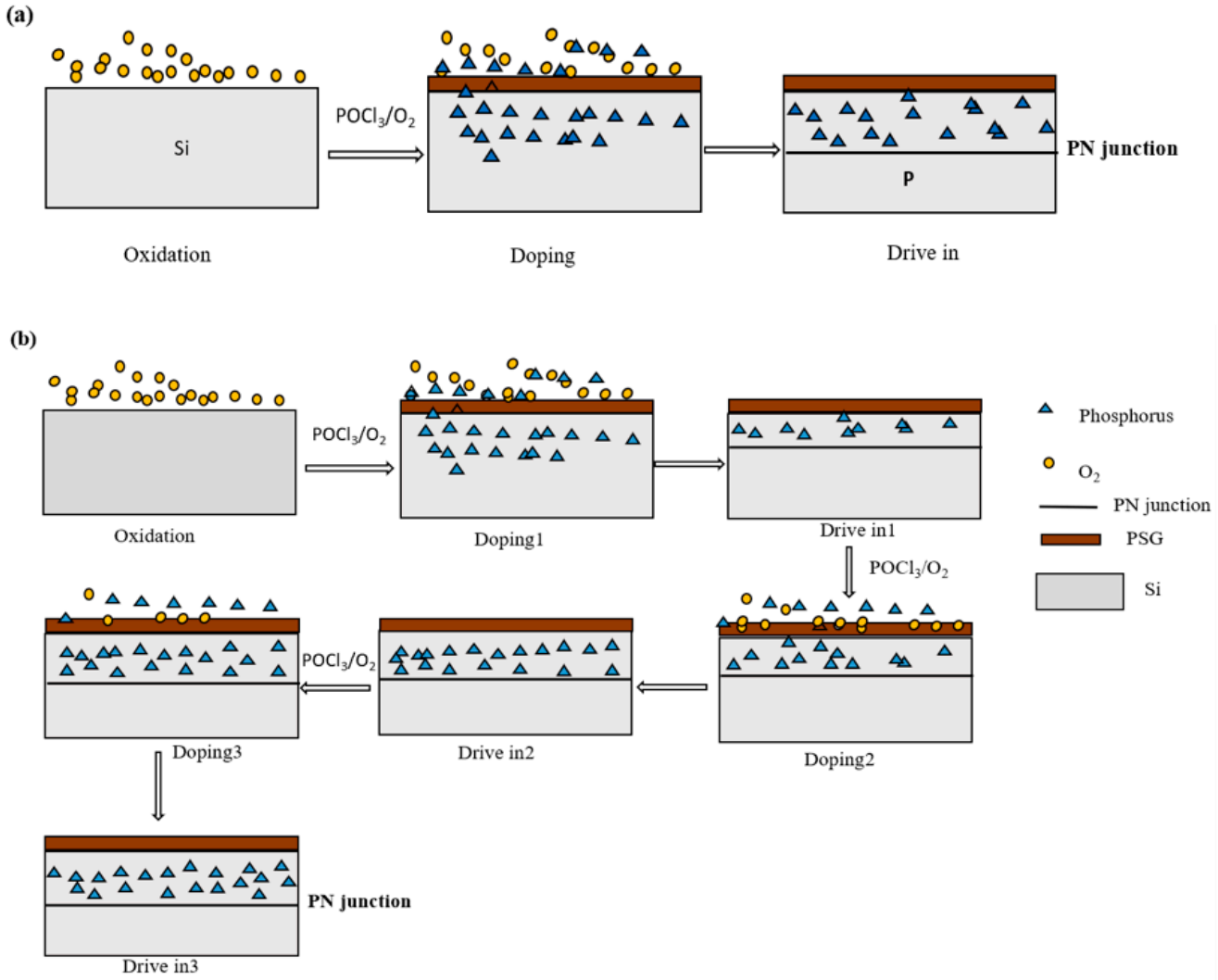

Figure 2. Schematic diagrams of the PN junction of solar cells obtained from (**a**) BKM and (**b**) LHL diffusion processes.

Figure 3 shows the sheet resistance box plots of solar cells and the ECV profiles of P doping for solar cells. The sheet resistance of solar cells was obtained (see Figure 3a). It can be observed that solar cells produced from LHL and BKM diffusion processes had the

same sheet resistance of about 90 Ω/sq. However, the sheet resistance of solar cells from the LHL process was much more uniform than that of the cells from the BKM diffusion process. The results indicated that the LHL process could be beneficial for the *FF* and the series resistance of solar cells [17]. Figure 3b presents the P doping profile of solar cells produced by LHL and BKM diffusion processes. The solar cells obtained from the LHL diffusion process had a lower surface concentration of P doping, approximately 4.54×10^{20} fewer atoms/cm^3 than those produced from the BKM diffusion process, which produced about 6.08×10^{20} atoms/cm^3 at the junction depth of about 0.02 µm. For LHL and BKM diffusion processes, the solar cells had the same junction depth of around 0.3 µm at a dopant concentration of $N = 10^{17}$ atoms/cm^3. During emitter formation and at high phosphorus concentrations, precipitates were formed on the silicon surface and promoted the existence of electrically inactive phosphorus which formed a dead layer at the silicon surface. This behavior is characterized by a kinked shape in the experimental profiles. This kink has a great impact on solar cell performance since it results in low collection efficiency near the front surface.

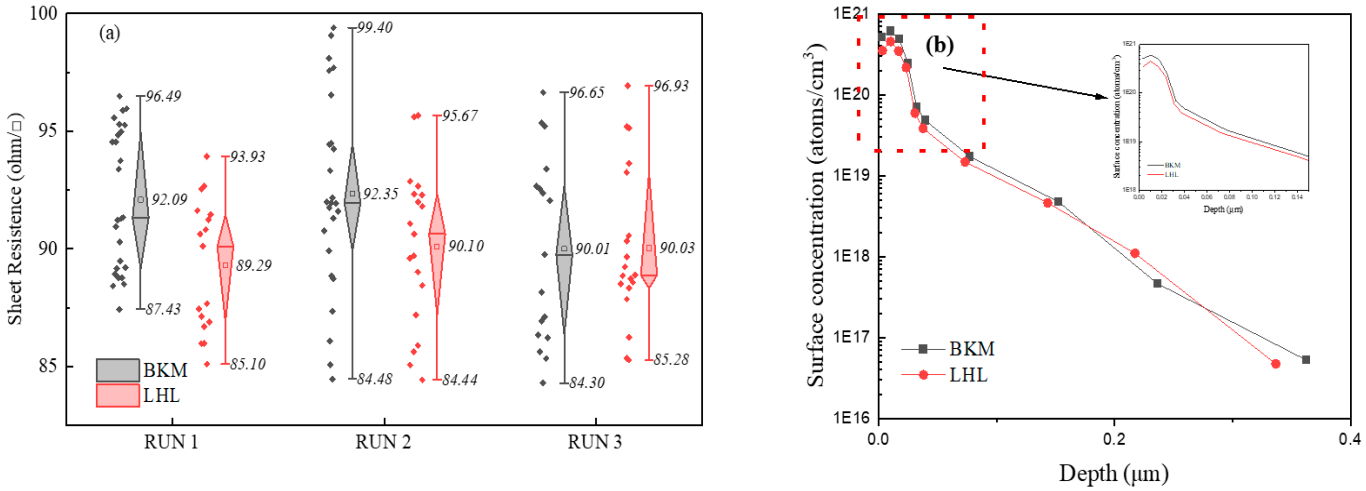

Figure 3. Sheet resistance box-plots of solar cells obtained from BKM and LHL diffusion processes (**a**), and the ECV profiles of P doping (**b**).

In the module of PV solar cell marketing, only the V_{oc} and *FF* values have more advantages on the power. In this study, the advantage of the LHL diffusion process could be beneficial to the increase in V_{oc} and *FF* values. Table 2 displays the gap of electrical characteristics of solar cells obtained by LHL and BKM diffusion processes. The solar cells obtained from the LHL diffusion process have an increase in median V_{oc} value of about 1 mV, compared with the BKM diffusion process. This increase might be due to the low surface concentration of P doping (see Figure 4b). At the same time, the median *FF* value is increased by 0.30%, which can be contributed to the strong impurity absorption effect of Si wafers and the decrease in inactive phosphorus in the LHL diffusion process.

Table 2. The gap in electrical characteristics for solar cells obtained by LHL and BKM diffusion processes.

Condition		V_{oc} (V)	J_{sc} (mA)	R_{ser} (ohm)	*FF* (%)	E_{ff} (%)
Gap (LHL-BKM)	Run1	0.0012	−0.03	0.0000	0.27%	0.08%
	Run2	0.0012	−0.05	0.0000	0.36%	0.08%
	Run3	0.0006	−0.04	−0.0001	0.27%	0.1%
Average		0.0010	−0.04	0.0000	0.30%	0.09%

Note: V_{oc}: open circuit voltage; J_{sc}: short circuit current; R_{ser}: series resistance; *FF*: fill factor; E_{ff}: efficiency.

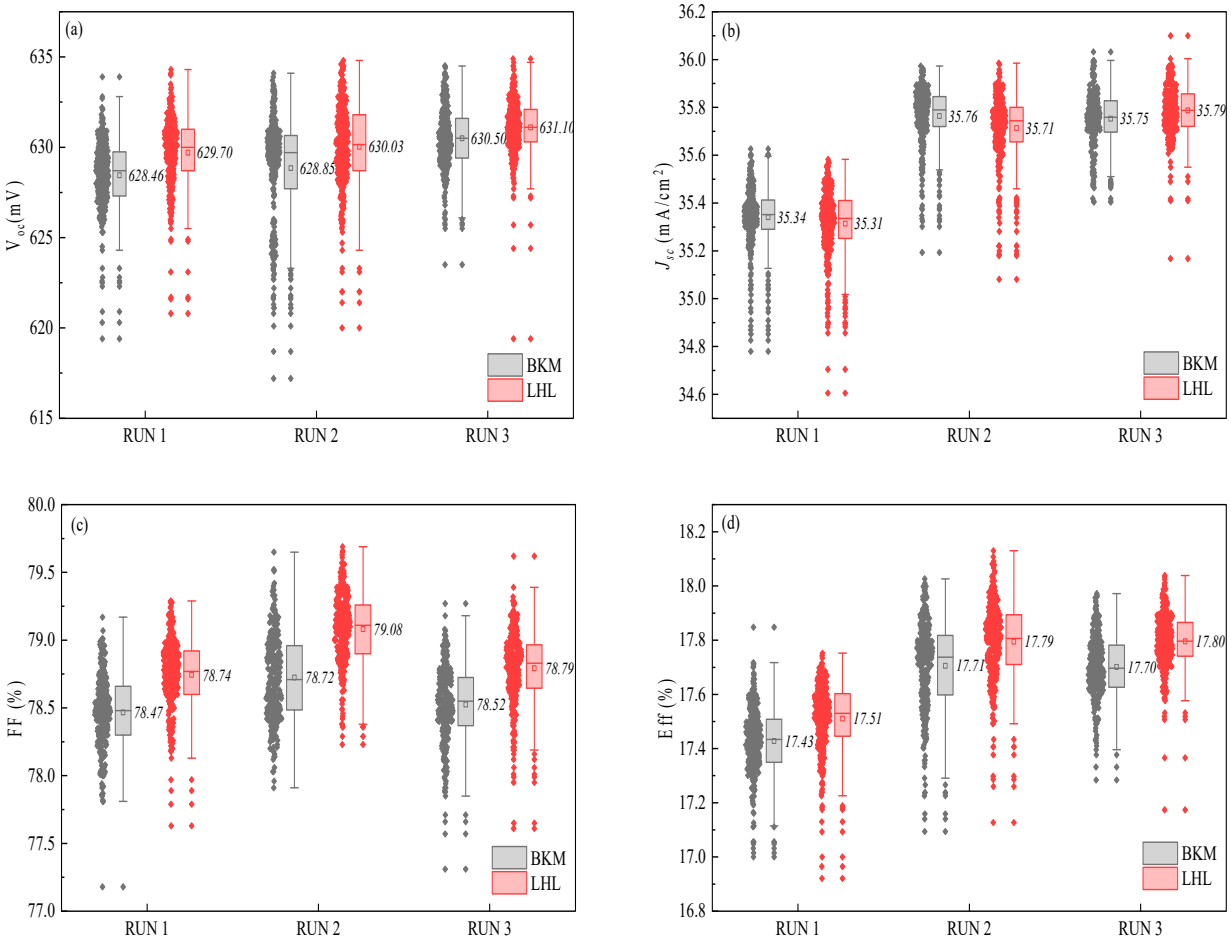

Figure 4. Box plots of the electrical characteristics of solar cells obtained from BKM and LHL diffusion processes (**a**) V_{oc}, (**b**) J_{sc}, (**c**) *FF*, and (**d**) E_{ff}.

Figure 4 shows the box plots of electrical characteristics of solar cells produced from BKM and LHL diffusion processes. The median V_{oc} values of the solar cells produced by LHL and BKM processes are 630 ± 1 mV and 629 ± 1 mV, respectively (see Figure 4a). For LHL and BKM diffusion processes, the median J_{sc} values of the solar cells are the same, about 35.55 ± 0.25 mA (see Figure 4b). The median FF values of the solar cells obtained by LHL and BKM diffusion processes are 78.9 ± 0.1% and 78.6 ± 0.1%, respectively (see Figure 4c). The median E_{ff} values of the cells produced by LHL and BKM diffusion processes are 17.65 ± 0.15% and 17.55 ± 0.15%, respectively (Figure 4d). The E_{ff} value of the solar cells from the LHL diffusion process is increased by 0.08–0.10%, which was mainly attributed to the increase in V_{oc} value of 1 mV and the *FF* value of 0.30%. These results show the convergence of the V_{oc}, *FF* and E_{ff} values of the solar cells obtained from the LHL diffusion process is better than the parameters of cells produced from the BKM diffusion process, which was attributed to the distribution and diffusion of impurities. At the same time, the effective doping concentration is effectively controlled, the generation of the dead layer is reduced, and recombination is reduced, resulting in the increase of the V_{oc} value. Furthermore, due to the LHL diffusion process with three-time temperature changes, it is more conducive to the precipitation of harmful impurities into the PSG layer, which improves the service life of the bulk, thus resulting in the improvement of *FF* values. The increase in Voc and FF can be explained by active phosphorus atoms and the optimized contact-formation process. Table S1 summarizes the performance of solar cells doped P by different diffusion processes (see Supplementary Material).

Figure 5 presents the typical top-view SEM micrographs of the front side of solar cells. It shows that the front busbar is of uniform height: about 12.4 µm (see Figure 5a), and the

height of the front finger is also smooth: about 24.3 μm (see Figure 5b). However, the Ag paste does not uniformly corrode the P doping layer. In Figure 5c, the corroded depth is approximately 0.12 μm, so the effect of the surface concentration at the depth of 0.15 μm on the contact resistance (ρ_c) could be emphasized, which is important for the FF values. Figure 6 shows the contact resistivity of solar cells from two diffusion processes. The ρ_c values of the cells from LHK and BKM processes were 18.86 mΩ·cm^2 and 19.09 mΩ·cm^2. The LHL diffusion process has no additional costs. It would be a benefit for the large-scale industrial production of the P doping process of PV solar cells.

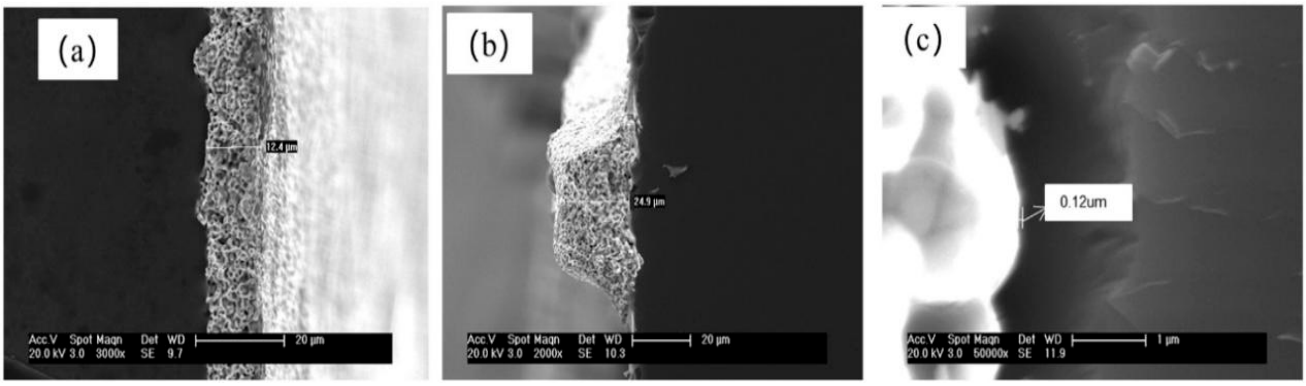

Figure 5. SEM images of (**a**) front busbar, (**b**) front finger, and (**c**) Ag-Si alloy.

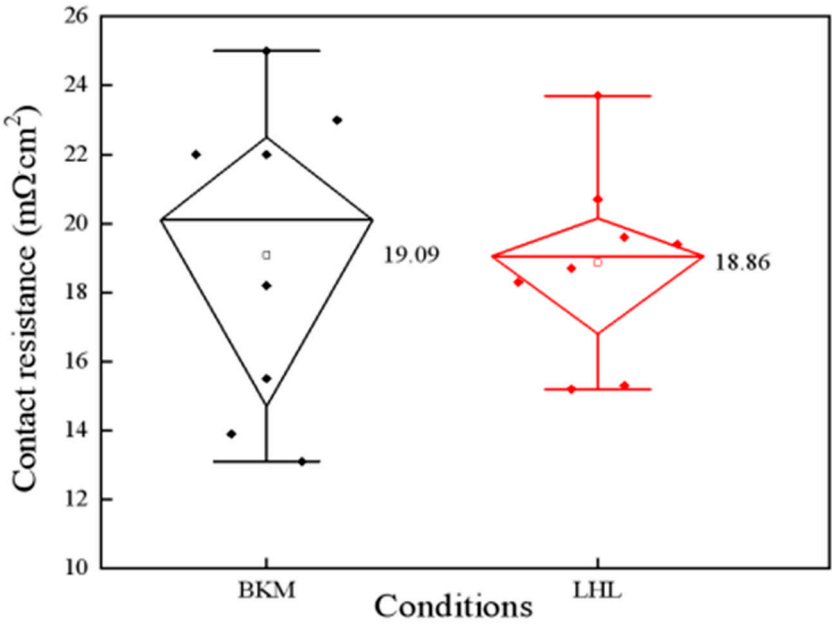

Figure 6. Contact resistivity of solar cells from LHL and BKM diffusion processes.

4. Conclusions

The non-uniformity of worm-shaped structures increases the difficulty of P diffusion. In addition, the phosphorus profile is highly affected by the tube furnace conditions. (Time and temperature must be considered carefully). A diffusion process featuring low-high-low temperature and three steps was used to diffuse P elements for solar cells with different $POCl_3$ flows in every step. This allows for systematic manipulation of doping profiles, especially for manipulation of the surface-active concentration of P doping, control of the doping depth, and reduction in the dead layer at the silicon surface, respectively. The solar cells with a low surface concentration of P doping of 4.54 × 10^{20} atom/cm^3 and junction depth of 0.31 μm at a dopant concentration of N = 10^{17} atoms/cm^3 were obtained. The

open-circuit voltage and FF values of solar cells increased up to 1 mV and 0.30%, compared with the online low-temperature diffusion process respectively, which can be contributed to the low surface concentration of P doping (decreasing inactive phosphorus) and the strong impurity absorption effect of Si wafers obtained from the low-high-low temperature diffusion process. The efficiency and the power of solar cells were increased by 0.1% and 1 W, respectively. The LHL diffusion process has no additional costs. It would be beneficial for the large-scale industrial production of the P doping process of PV solar cells.

Supplementary Materials: The following supporting information can be downloaded at: https://www.mdpi.com/article/10.3390/ma16051824/s1.

Author Contributions: X.X.: Data curation, Formal analysis, Investigation, Methodology; W.W.: Writing—original draft, Writing—review& editing, Supervision; Q.W.: Writing—review& editing. All authors have read and agreed to the published version of the manuscript.

Funding: This work has been partially supported by Jiangsu Province Cultivation base for State Key Laboratory of Photovoltaic Science and Technology (SKLPST 202201).

Informed Consent Statement: Not applicable.

Data Availability Statement: The data presented in this study are available upon request from the corresponding author.

Conflicts of Interest: We declare that we do not have any commercial or associative interests that represent a conflict of interest in connection with the work submitted.

References

1. Lee, S.H.; Min, K.H.; Choi, S.; Song, H.; Kang, M.G.; Kim, T.; Park, S. Advanced carrier lifetime analysis method of silicon solar cells for industrial applications. *Sol. Energy Mater. Sol. Cells* **2023**, *251*, 112144. [CrossRef]
2. Bennett, N.S.; Wight, N.M.; Popuri, S.R.; Bos, J.G. Efficient thermoelectric performance in silicon nano-films by vacancy-engineering. *Nano Energy* **2015**, *16*, 350–356. [CrossRef]
3. Kumar, P.; Pfeffer, M.; Willsch, B.; Eibl, O. Contact formation of front side metallization in p-type, single crystalline Si solar cells: Microstructure, temperature dependent series resistance and percolation model. *Sol. Energy Mater. Sol. Cells* **2016**, *145*, 358–367. [CrossRef]
4. Ghembaza, H.; Zerga, A.; Saïm, R. Efficiency improvement of crystalline silicon solar cells by optimizing the doping profile of $POCl_3$ diffusion. *Inter. J. Sci. Technol. Res.* **2014**, *3*, 1–5. [CrossRef]
5. Wolf, A.; Kimmerle, A.; Werner, S.; Maier, S.; Belledin, U.; Meier, S.; Biro, D. Status and perspective of emitter formation by $POCl_3$-diffusion. In Proceedings of the 31st European Photovoltaic Solar Energy Conference and Exhibition, Hamburg, Germany, 14–18 September 2015; pp. 414–419.
6. Khedher, N.; Hajji, M.; Hassen, M.; BenJaballah, A.; Ouertani, B.; Ezzaouia, H.; Bessais, B.; Selmi, A.; Bennaceur, R. Gettering impurities from crystalline silicon by phosphorus diffusion using a porous silicon layer. *Sol. Energy Mater. Sol. Cells* **2005**, *87*, 605–611. [CrossRef]
7. Shabani, M.; Yamashita, T.; Morita, E. Study of gettering mechanisms in silicon: Competitive gettering between phosphorus diffusion gettering and other gettering sites. *Solid State Phenom.* **2008**, *131–133*, 399–404.
8. Dastgheib-Shirazi, A.; Steyer, M.; Micard, G.; Wagner, H.; Altermatt, P.P.; Hahn, G. Relationships between Diffusion Parameters and Phosphorus Precipitation during the POCl3 Diffusion Process. *Energy Procedia* **2013**, *38*, 254–262. [CrossRef]
9. Kittidachachan, P.; Markvart, T.; Ensell, G.; Greef, R.; Bagnall, D. An analysis of a "dead layer" in the emitter of n/sup +/pp/sup +/ solar cells. In Proceedings of the Thirty-first IEEE Photovoltaic Specialists Conference, Lake Buena Vista, FL, USA, 3–7 January 2005; pp. 1103–1106. [CrossRef]
10. Book, F.; Dastgheib-Shirazi, A.; Raabe, B.; Haverkamp, H.; Hahn, G.; Grabitz, P. Detailed analysis of high sheet resistance emitters for selectively doped silicon solar cells. In Proceedings of the 24th European Photovoltaic Solar Energy Conference, Hamburg, Germany, 21–25 September 2009. [CrossRef]
11. Saule, W.; Delahaye, F.; Queisser, S.; Wefringhaus, E.; Schweckendiek, J.; Nussbaumer, H. High efficiency inline diffusion process with wet-chemical emitter etch-back. In Proceedings of the 24th European Photovoltaic Solar Energy Conference, Hamburg, Germany, 21–25 September 2009. [CrossRef]
12. Ostoja, P.; Guerri, S.; Negrini, P.; Solmi, S. The effects of phosphorus precipitation on the open-circuit voltage in N^+/P silicon solar cells. *Sol. Cells* **1984**, *11*, 1–12. [CrossRef]
13. Nobili, D. Precipitation as the phenomenon responsible for the electrically inactive phosphorus in silicon. *J. Appl. Phys.* **1982**, *53*, 1484–1491. [CrossRef]

14. Li, H.; Ma, F.-J.; Hameiri, Z.; Wenham, S.; Abbott, M. On elimination of inactive phosphorus in industrial $POCl_3$ diffused emitters for high efficiency silicon solar cells. *Sol. Energy Mater. Sol. Cells* **2017**, *171*, 213–221. [CrossRef]
15. Cui, M.; Jin, C.; Yang, Y.; Wu, X.; Zhuge, L. Emitter doping profiles optimization and correlation with metal contact of multi-crystalline silicon solar cells. *Optik* **2016**, *127*, 11230–11234. [CrossRef]
16. Cho, E.; Ok, Y.-W.; Dahal, L.; Das, A.; Upadhyaya, V.; Rohatgi, A. Comparison of POCl3 diffusion and phosphorusion-implantation induced gettering in crystalline Si solar cells. *Sol. Energy Mater. Sol. Cells* **2016**, *157*, 245–249. [CrossRef]
17. Ghembaza, H.; Zerga, A.; Saïm, R.; Pasquinelli, M. Optimization of Phosphorus Emitter Formation from POCl3 Diffusion for p-Type Silicon Solar Cells Processing. *Silicon* **2016**, *10*, 377–386. [CrossRef]
18. Li, H.; Kim, K.; Hallam, B.; Hoex, B.; Wenham, S.; Abbott, M. POCl3 diffusion for industrial Si solar cell emitter formation. *Front. Energy* **2017**, *11*, 42–51. [CrossRef]
19. Chen, J.; Xi, Z.; Wu, D.; Yang, D. Effect of variable temperature phosphorous gettering treatments on the performance of multicrystalline silicon. *Acta Energ. Sol. Sin.* **2017**, *28*, 160–164. [CrossRef]
20. Chen, Y.; Hao, Q.; Liu, C.; Zhao, J.; Wu, D.; Wang, Y. Effect of transition-metal contamination on minority lifetime in cast multi-crystalline silicon under rapid thermal processing. *Acta Energ. Sol. Sin.* **2019**, *30*, 611–614. [CrossRef]
21. Ural, A.; Griffin, P.B.; Plummer, J.D. Fractional contributions of microscopic diffusion mechanisms for common dopants and self-diffusion in silicon. *J. Appl. Phys.* **1999**, *85*, 6440–6446. [CrossRef]
22. Rousseau, P.M.; Griffin, P.B.; Fang, W.T.; Plummer, J.D. Arsenic deactivation enhanced diffusion: A time, temperature, and concentration study. *J. Appl. Phys.* **1998**, *84*, 3593–3601. [CrossRef]